Polymer Journal, Vol. 19, No. 8, pp 951—963 (1987)

Reversing-Pulse Electric Birefringence of Poly(γ-benzyl L-glutamate) IV. Electric, Optical, and Hydrodynamic Properties in Helix-Forming Solvents as Evaluated from Field-On and Field-Off Processes†

Kiwamu YAMAOKA,* Shinobu YAMAMOTO, and Isao KOSAKO

Faculty of Science, Hiroshima University, Higashisenda-machi, Naka-ku, Hiroshima 730, Japan

(Received March 5, 1987)

ABSTRACT: Reversing-pulse electric birefringence (RPEB) of poly(γ-benzyl L-glutamate), $[Glu(OBzl)]_n$, with a weight-average molecular weight of 1.71×10^5 was measured at 20°C and at 535 nm in four helix-forming solvents: 2-chloroethanol, cyclohexanone, pyridine, in which $[Glu(OBzl)]_n$ is dissolved molecularly, and chloroform in which it is aggregated. A standard analytical procedure is given for the RPEB signal which represents the field-on and field-off processes. The steady-state birefringence of $[Glu(OBzl)]_n$ was measured over a wide field strength range up to *ca.* 20 kV cm^{-1}. The Kerr law was obeyed at low fields, while a saturating trend was observed at higher fields. Specific and intrinsic Kerr constants were obtained. The weight-average molecular length l_w, the degree of polydispersity l_w/l_n, and the electric parameter $(\beta_w)^2/2\gamma_w$ were evaluated from the reverse-transient signal which exhibits a deep minimum. The values of l_w and l_w/l_n in the field-off process were also evaluated from the birefringence-average relaxation time and initial slope, both of which were obtained from the decay signal. The axial translation per residue of the $[Glu(OBzl)]_n$ helix was found to range between 1.27 and 1.30 Å at dilute concentrations regardless of solvent.

KEY WORDS Reversing-Pulse Electric Birefringence / Poly(γ-benzyl L-glutamate) / Solution Conformation / Electrooptical Properties / Relaxation Time /

In the original work on light scattering and viscosity in *N*,*N*-dimethylformamide and in chloroform–formamide mixture, poly(γ-benzyl L-glutamate), $[Glu(OBzl)]_n$, was reported to be in the α-helix form.[2] Later studies, however, have not necessarily supported this conclusion; some different helical conformations have been proposed for $[Glu(OBzl)]_n$,[3-7] which is considered to be a standard for many rodlike polypeptides and proteins. The major source for this disagreement arises from the uncertainty in the relationship between the absolute molecular weight and chain length. The problems may be attributed to the following: (1) experimental difficulties inherently associated with light scattering and differential refractive index measurements,[8,9] (2) the polydispersity of molecular weight of $[Glu(OBzl)]_n$ samples,[5] (3) the dependence of chain flexibility on molecular weights,[7,10] (4) the interhelix interaction leading to aggregate formation,[8,9,11] and (5) the approximations made for estimating the axial ratio, radius, and hydrodynamic volume of $[Glu(OBzl)]_n$ from viscometric measure-

† This work was in part presented at the 32nd meeting of the Society of Polymer Science, Japan held at Kanazawa, October 1983.[1]

* To whom correspondence should be addressed.

ments.[12]

Pulsed electric birefringence is a direct method for clarifying the electrical and hydrodynamic properties of rodlike polypeptides;[7,13-21] thus, it can resolve some of the above problems. The reversing-pulse electric birefringence (RPEB) technique[22] is unique in the sense that the field orientation mechanism, the rotary diffusion coefficient, and the molecular weight (or length) distribution of solutes may be evaluated from measurements in the low electric field strength region.[23] The radius and axial translation per residue can be estimated from RPEB measurements together with the intrinsic viscosity and the molecular weight. Hence, the conformation of rodlike polymers in solution can be resolved.[24,25] Experimental results of electric birefringence have usually been interpreted under the implicit assumption that the externally applied electric field can orient the solute molecules without inducing any direct field effects (*e.g.*, association-dissociation or conformational transition), unless birefringence signals indicate some visible anomalies.[15] However, a recent RPEB study of poly(γ-methyl L-glutamate) in hexafluoro-2-propanol clarified in detail that a structural transition is induced by an applied electric pulse of low field strength in the course of the field orientation of the helix.[26-28] In transient electric birefringence studies, therefore, it is imperative to first ascertain the absence of the direct electric field effect on macromolecular conformation.[28]

Aiming at further developments of RPEB techniques,[23-29] we report in this paper an RPEB study of the solution conformation of $[Glu(OBzl)]_n$ with particular attention to the aforementioned direct field effect. For this purpose, we used a fractionated and only slightly polydisperse sample in four helix-forming solvents;[11] 2-chloroethanol, cyclohexanone, pyridine, in which $[Glu(OBzl)]_n$ is nearly or completely unaggregated, and chloroform in which the polymer forms an aggregated helix. Experiments were pursued, on a comparative basis, both in the field-on processes (reverse-transient and steady-state birefringence) and in the field-off process (decay). Discussion is presented on possible differences in molecular conformation and electrooptical properties of $[Glu(OBzl)]_n$ between these two processes.

EXPERIMENTAL

Materials

A sample of $[Glu(OBzl)]_n$ with a weight-average molecular weight $\bar{M}_w$ of 1.9×10^5 was dissolved in dichloromethane and fractionated into three fractions with methanol by the successive precipitation method.[30] The smallest-molecular-weight fraction was used in this work. The intrinsic viscosity, $[\eta]$, was measured in *N*,*N*-dimethylformamide at 20°C with a Ubbelohde-type dilution viscometer at a flow time of 267.6 s.[24,25] The value of $\bar{M}_w$ was estimated to be 1.71×10^5 from the $[\eta]$ value of 228.4 $cm^3\,g^{-1}$ with the relationship given by Doty *et al.*[2] Reagent-grade pyridine and UV-spectrograde chloroform (Dōjindo Labs.) were used without further purification. Reagent-grade 2-chloroethanol (Wakō Chemicals) was treated with anhydrous sodium carbonate overnight, and distilled under reduced pressure at 40°C, nitrogen gas being introduced, and kept under nitrogen atmosphere. Reagent-grade cyclohexanone (Katayama Chemicals) was distilled under reduced pressure prior to use. The solution of $[Glu(OBzl)]_n$ was prepared by weighing the anhydrous sample dried at 78°C for 8 h under reduced pressure. The concentration of solution was expressed in terms of the residue concentration C_p in mM ($=10^{-3}$ mol dm^{-3}) or of the mass concentration c in g cm^{-3}.

RPEB Measurements

Electric birefringence was measured at 535 nm and 20°C on an apparatus built in this laboratory.[23,29] For RPEB signals measure-

ments, a reversing-pulse generator with a time constant of 0.5 μs each for the buildup, reverse, and decay portion was used in the low field strength region ($E \leq 6\,kV\,cm^{-1}$). A quarter-wave plate was inserted in the optical path. A square-wave pulse generator with a time constant of *ca.* 0.7 μs was used for the steady-state and decay signal measurements in the medium-to-high field strength region ($E \leq 20\,kV\,cm^{-1}$) usually without the quarter-wave plate.[31]

Figure 1 shows a schematic diagram of the optical system and the acquisition and processing of birefringence signals. For the signal detecting system, a two-channel transient wave memory (Riken Denshi Co., Model TCH-4000(S) with the fastest sampling time of 50 ns/word, 8 bit, 4000 words)[27,28] was utilized in place of the oscilloscope formerly in use.[23-25] The photocurrent generated from a photomultiplier was fed to one channel and the attenuated electric pulse voltage to the other. The digitized signals were then transferred to a microcomputer (Oki Electric Co., IF 800 Model 10) with two minifloppy disk-drives *via* an interface. The desired numbers of RPEB signals were stored in the floppy disk and then averaged. Programs were written for the analyses of both the steady-state, reverse, and decay birefringence signals and the applied electric field strength. Figure 2 shows a digitized RPEB signal of $[Glu(OBzl)]_n$ in 2-chloroethanol; each dot is an average of two sampling times 2 μs apart. It is seen that a deep extremum or "dip" appears in the reverse process and the reverse-pulse duration is deliberately set longer than the first square pulse in order for the reverse signal to return completely to the original steady-state level.

The electric birefringence, $\Delta n = n_{\parallel} - n_{\perp}$, was expressed in terms of the observed optical phase retardation δ as $\delta = (2\pi d/\lambda)\Delta n$, where λ is the wavelength *in vacuo* and d is the optical path length. Two Kerr cells of cylindrical type made of Kel-F were used,[17,31] the electrode gaps being 0.207 cm ($d = 1.00$ cm) and 0.330 cm

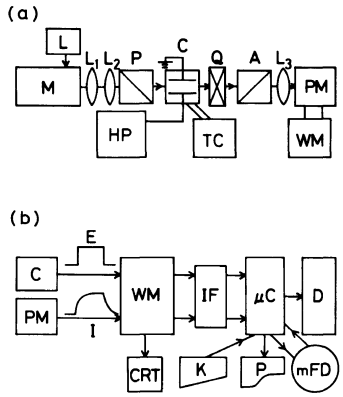

Figure 1. Schematic diagrams of (a) the optical system and (b) the data acquisition and processing system for RPEB signals. (a) L, 150 W iodine-quartz lamp; L_1, L_2, and L_3, lenses; M, prism UV-VIS monochromator; P, Glan–Thompson polarizer; C, Kerr cell; Q, quarter-wave plate made of quartz; A, Glan–Thompson analyzer; PM, Hamamatsu R-376 head-on photomultiplier; HP, two-channel high voltage pulse generator; TC, temperature control; WM, transient wave memory. (b) E, attenuated electric pulse; I, photocurrent; CRT, monitor oscilloscope; IF, interface; μC, microcomputer; P, printer; mFD, minifloppy disk drives; K, key board; D, display.

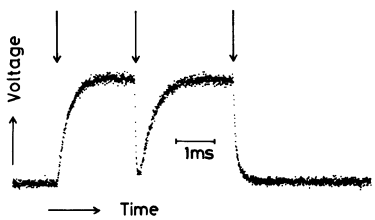

Figure 2. A digitized RPEB signal of $[Glu(OBzl)]_n$ in 2-chloroethanol at 20°C. Arrows indicate the application, reversal and removal of an external electric pulse field. Concentration: 1.12 mM; Field strength: 3.63 $kV\,cm^{-1}$. 25 signals were averaged.

($d = 2.00$ cm). The phase retardation of each solvent, $\delta_{solvent}$, was subtracted from the values of δ observed for $[Glu(OBzl)]_n$ solutions, $\delta_{[Glu(OBzl)]_n} = \delta_{obsd} - \delta_{solvent}$, whenever this correction was needed. The Kerr constant B ($= (1/\lambda)(\Delta n/E^2)_{E\to 0} = (1/2\pi d) \times (\delta/E^2)_{E\to 0}$) of each solvent in cmV^{-2} was determined to be 7.58×10^{-12} (2-chloroethanol), 2.03×10^{-11} (cyclohexanone), 2.81×10^{-11} (pyridine),

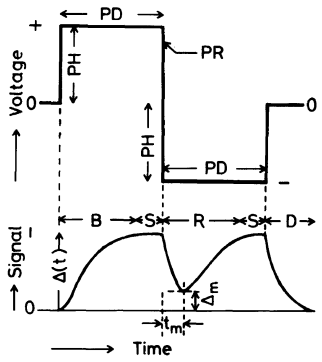

Figure 3. Illustration of RPEB signal and applied electric pulse field. PH, pulse height; PD, pulse duration; PR, pulse reversal; B, buildup process; R, reverse process; D, decay process; S, steady state; $\Delta(t)$, normalized birefringence; t_m, time required for the extremum Δ_m.

and -4.00×10^{-12} (chloroform).

Analysis of Birefringence Data

The detailed analytical procedure has been given elsewhere for the birefringence signals of nonaqueous solutions containing rodlike, nonconducting polymer molecules which are polydispersed with respect to the molecular length l.[23-23,32] Therefore, the minimum number of theoretical expressions is given below. Figure 3 shows the RPEB signal and pulse pattern with nomenclature currently in use for data analysis.

(1) *Field-On Processes.*

(i) *Steady or Equilibrium State.* The steady-state birefringence $\Delta n(\infty)$ at an arbitrary field strength E is expressed with the weight-average orientation function $\langle\Phi\rangle_w$ as

$$\Delta n(\infty)=\int_0^\infty \Delta n(\infty,l)\,dl=\frac{2\pi\bar{C}_v\Delta g}{n}\langle\Phi(\beta(l),\gamma(l))\rangle_w$$
$$=\frac{2\pi\bar{C}_v\Delta g}{n}\frac{\int_0^\infty \Phi((\beta(l),\gamma(l))lf_n(l)\,dl}{\int_0^\infty lf_n(l)\,dl} \quad (1)$$

(ii) *Reverse Transient.* In the low field region where the Kerr law holds, the normalized RPEB signal $\Delta_R(t)$ is given as

$$\Delta_R(t)\equiv\frac{\Delta n(t)}{\Delta n(\infty)}=\frac{\int_0^\infty \Delta n(\infty,l)\left(1-\frac{3\beta(l)^2}{\beta(l)^2+2\gamma(l)}[\exp(-2\Theta_{11}(l)t)-\exp(-6\Theta_{11}(l)t]\right)dl}{\int_0^\infty \Delta n(\infty,l)\,dl} \quad (2)$$

(2) *Field-Off Process.*

(i) *Decay.* The normalized birefringence decay signal $\Delta_D(t)$ after removal of the applied pulse field at an arbitrary strength is given as

$$\Delta_D(t)\equiv\frac{\Delta n(t)}{\Delta n(\infty)}=\frac{\int_0^\infty \Delta n(\infty,l)\exp(-6\Theta_{11}(l)t)\,dl}{\int_0^\infty \Delta n(\infty,l)\,dl} \quad (3)$$

Notations are as follows: $\Phi(\beta(l),\gamma(l))$ is the "classical orientation function," in which $\beta(l)^2/2\gamma(l)>0$, for thin rodlike polymer solutes.[13] n is the refractive index of solution. $\bar{C}_v$ is the volume fraction of solute. $\Delta g=(g_3-g_1)$ is the optical anisotropy factor independent of length l for a long polymer molecule.[33] $\beta(l)=\mu(l)E/kT$ and $\gamma(l)=\Delta\alpha(l)E^2/2kT$, where $\mu(l)$ is the permanent electric dipole moment, $\Delta\alpha(l)=(\alpha_{33}-\alpha_{11})$ is the covalent (atomic and electronic) polarizability anisotropy, k is the Boltzmann constant, and T is the absolute temperature. $\Theta_{11}(l)$ is the rotary diffusion coefficient of the solute around the transverse axis. $\Delta n(\infty,l)\equiv(2\pi\bar{C}_v/15n)\Delta g\phi(l)\{\beta(l)^2+2\gamma(l)\}$ in the Kerr-law region; $\phi(l)$ is the fraction of molecules with length l, which is proportional to $lf_n(l)$, and $f_n(l)$ is the probability density function based on the number of solutes in solution.[23]

Since the type of distribution function is not too critical for a well-fractionated sample,[24,25]

the Lansing–Kraemer distribution function[34] is assumed for the length of the $[Glu(OBzl)]_n$ helix:

$$f_n(l)=(1/\omega l\sqrt{\pi})\exp[-(\ln(l/l_L)^2/\omega^2)] \quad (4)$$

where ω and l_L are the parameters related as $l_w=l_L(l_w/l_n)^{3/2}$ and $l_w/l_n=\exp(\omega^2/2)$. The degree of polydispersity is defined as the ratio of weight-average, l_w, to number-average, l_n, lengths, l_w/l_n, for helical polymer molecules whose molecular weights are proportional to length.

RESULTS AND DISCUSSION

Field-On Processes

Steady-State Birefringence of $[Glu(OBzl)]_n$. Figure 4 shows the specific steady-state birefringence per path length, δ/cd, of $[Glu(OBzl)]_n$ in four solvents. In all cases, the values of δ/cd approach a saturation at higher fields, the sign always being positive, while they are proportional to the square of field strength in the low field region, indicating that the Kerr law is obeyed. In 2-chloroethanol, cyclohexanone, and pyridine, in which the $[Glu(OBzl)]_n$ helix was reported to be either molecularly dispersed or only slightly aggregated,[11] δ/cd values are almost independent of concentration (Figure 4a). This result reveals that the solute helix is stable in the concentration range of 4—1 mM, without being affected by externally applied electric fields. On the other hand, δ/cd values in chloroform show a marked dependence on concentration (Figure 4b). At higher concentrations, the signal heights decrease progressively by repetitive pulses of high electric field strength. Thus, in the field-on process where the solutes are oriented, the electrooptical properties of $[Glu(OBzl)]_n$ helices in chloroform are affected by the applied field. The electric field induces either the dissociation of aggregated helices[11,21] or the irreversible transition.

Specific Kerr Constant. The specific Kerr constant, B/c (c being in g cm^{-3}), is defined as

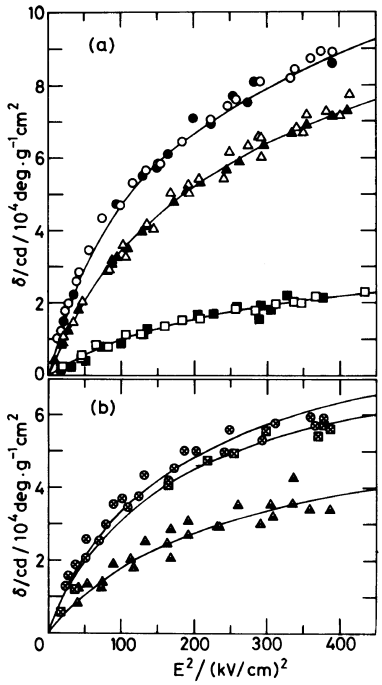

Figure 4. Field-strength dependence of the specific steady-state optical phase retardation per path length, δ/cd, at 20°C. (a) 2-chloroethanol (△, 1.12 mM; ▲, 0.56 mM), cyclohexanone (○, 4.27 mM; ●, 1.54 mM), and pyridine (□, 2.08 mM; ■, 1.04 mM). (b) chloroform (⊠, 3.19 mM; ⊗, 1.91 mM, ⧋, 0.957 mM). Solid lines are curves theoretically calculated with the parameters in Table I.

$$\frac{B}{c}=\frac{1}{\lambda}\left(\frac{\Delta n}{cE^2}\right)_{E\to 0}=\frac{1}{2\pi d}\left(\frac{\delta}{cE^2}\right)_{E\to 0} \quad (5)$$

Figure 5 shows plots of observed values of δ/cdE^2 against the square of field strength at low fields for each solvent. The plots indicate that δ/cdE^2 values increase slightly in the low field region ($E\leq 6$ kV cm^{-1}), but show no maximum at extremely low fields. This field strength dependence is an indication that $\beta^2/2\gamma\gtrsim 2$.[13] The values of δ/cdE^2 extrapolated to zero field give rise to the specific Kerr constant B/c. By extrapolation of B/c values to zero concentration, the intrinsic Kerr constants, $[B/c]_{c\to 0}$, were evaluated for three solvents and are given in Table I. In chloroform, B/c values show a marked concentration dependence, and the $[B/c]_{c\to 0}$ value is difficult to

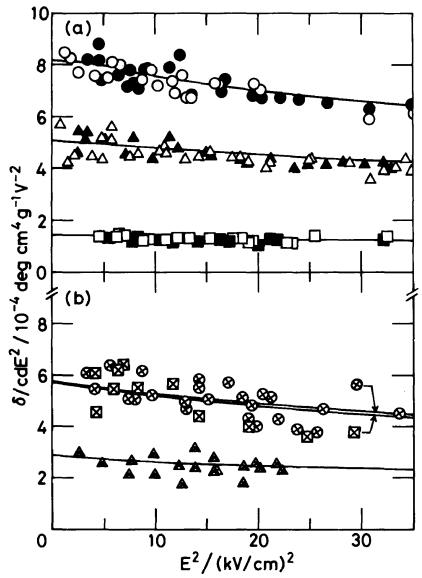

Figure 5. Field-strength dependence of δ/cdE^2 in four helix-forming solvents in the low field strength region. (a) 2-chloroethanol (△, ▲), cyclohexanone (○, ●), and pyridine (□, ■). (b) chloroform (⊠, ⊗, ⧋). Concentrations are the same as those in Figure 4. Solid lines are theoretical (*cf.* Figure 4).

determine. This is most likely due to the dissociation of aggregated helices with decreasing concentrations rather than conformational transition.[11]

The intrinsic Kerr constant for a solution that contains rodlike $[Glu(OBzl)]_n$ molecules of various lengths is written as

$$\left[\frac{B}{c}\right]_{c\to 0}=\left(\frac{2\pi}{15\lambda\rho}\right)\left(\frac{\Delta g}{n}\right)\left[\frac{\langle\mu^2\rangle_w}{(kT)^2}+\frac{\langle\Delta\alpha\rangle_w}{kT}\right] \tag{6}$$

where $\langle\mu^2\rangle_w$ is the weight-average of the square of permanent dipole moment, $\langle\Delta\alpha\rangle_w$ is the weight-average polarizability anisotropy, and ρ is the density of solute. $\langle\mu^2\rangle_w$ is equal to $\langle\mu\rangle_z\langle\mu\rangle_w$, if $\mu(l)$ is proportional to l, which is the case for the rodlike $[Glu(OBzl)]_n$ helix with the average length less than 1200 Å.[24] The quantity $\langle\mu^2\rangle_w$ or $\langle\mu\rangle_z\langle\mu\rangle_w$ in eq 6 can be converted to $\langle\mu\rangle_w^2$ without any difficulty, when the distribution function $f_n(l)$ is specified for the rigid, rodlike molecule system.[23-25] Hereafter, the weight-average quantities will be denoted without symbol $\langle\ \rangle$, *e.g.*, μ_w for $\langle\mu\rangle_w$, whenever no confusion occurs. Equation 6 indicates that the intrinsic Kerr constant is the product of the optical term $(\Delta g/n)$ and the electric term $[(\mu^2{}_w/k^2T^2)+(\Delta\alpha_w/kT)]$. It should be noted that these two terms can never be evaluated separately from the steady-state birefringence measurement in the low field strength region.

In order to estimate the optical term, the saturated steady-state birefringence Δn_s must be obtained. The extrapolation of δ/cd values to infinitely high field would yield the Δn_s value, since the orientation function $\Phi(\beta,\gamma)$ approaches unity.[13] This extrapolation procedure is, however, often impractical, unless the δ/cd data at sufficiently high fields are available. This is because the curvature to extrapolation varies with the ratio of $\beta^2/2\gamma$, *i.e.*, $\mu^2/kT\Delta\alpha$. Another procedure (the curve-fitting method) has also been used to separate the optical term.[14,23-27] (This procedure will be discussed in a later section.) In this case, the polydispersity of a particular sample solution must be known in advance or independently, in order to draw theoretical "master curves" (*i.e.*, Φ_w *vs.* $(\beta_w)^2+2\gamma_w$ plots) to which an experimental δ/cd *vs.* E^2 plot is fitted ($(\beta_w)^2=(\mu_wE/kT)^2$ and $2\gamma_w=\Delta\alpha_wE^2/kT$). Fortunately, the degree of polydispersity, l_w/l_n, can be estimated from the reverse-transient signal with the assumption of an appropriate distribution function $f_n(l)$,[23-25] as shown in the next section.

Reverse-transient of $[Glu(OBzl)]_n$. The extremum in the reverse process of an RPEB signal is characterized by the time required for the signal to reach the extremum, t_m, and the normalized signal height from the baseline, Δ_m, at t_m (*cf.* Figure 3).[22] Figure 6 shows values of both Δ_m and t_m plotted against E^2. By extrapolation of these values to zero field strength, the limiting values, $(\Delta_m)_{E\to 0}$ and $(t_m)_{E\to 0}$, could be evaluated and are given in Table I. The value of $(\Delta_m)_{E\to 0}$ is related to the

Table I. Electrooptical and hydrodynamic properties of [Glu(OBzl)]$_n$ in four helix-forming solvents as evaluated from field-on processes at 20°C

Solvents[a]	$[B/c]_{c\to 0}$ / 10^{-6} cm^4 g^{-1} V^{-2}	$(\Delta_m)_{E\to 0}$	$(t_m)_{E\to 0}$ / μs	l_w / Å	l_w/l_n	$\beta_w^2/2\gamma_w$	μ_w[b] / D	$\Delta\alpha_w$[b] / 10^{-17} cm^3	$\Delta g/n$ / 10^{-3}
CEL	1.41	0.056	78.9	980	1.06	20.5	2720	0.89	4.2
CHN	2.28	0.068	64.5	1060	1.06	15.2	3370	1.84	4.7
PYN	0.37	0.149	26.9	1040	1.07	5.6	2620	3.03	1.1
CFM	1.59 (3.19)[c]	0.197	33.5	1330	1.14	6.8	3380	4.16	2.7
	1.58 (1.91)[c]	0.168	30.3	1280	1.10	9.9	3320	2.76	3.1
	0.83 (0.97)[c]	0.096	22.4	1160	1.08	20.5	2590	0.81	2.6

[a] CEL, 2-chloroethanol (3.43); CHN, cyclohexanone (2.22); PRN, pyridine (0.952); CFM, chloroform (0.568). Numerals in parentheses are the viscosity in centipoise at 20°C.

[b] 1D = 3.336×10^{-30} Cm and 1 cm^3 × 1.113×10^{-16} Fm^2.

[c] This value is B/c at the molar concentration C_p in mM specified in parentheses.

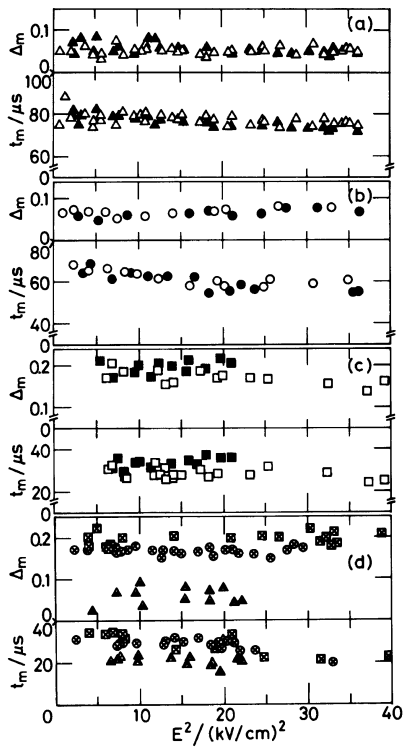

Figure 6. Field-strength dependence of the minimum position, Δ_m and t_m, in the reverse-transient signal of [Glu(OBzl)]$_n$. (a) 2-chloroethanol, (b) cyclohexanone, (c) pyridine, and (d) chloroform. Symbols are the same as those in Figure 4.

ratio of $(\beta_w)^2/2\gamma_w$, *i.e.*, $(\mu_w)^2/kT\Delta\alpha_w$, and hence, to the mechanism of electric field orientation and the helical structure of [Glu(OBzl)]$_n$.[22,23] Qualitatively, the larger the value for the depth, *i.e.*, $1-\Delta_m$, the greater is the contribution of the permanent electric dipole moment to the field orientation.[22-27] The value of the depth is larger in 2-chloroethanol and cyclohexanone ($\Delta_m \simeq 0.06$—0.08) than in pyridine ($\Delta_m \simeq 0.15$). In chloroform, the value of Δ_m lowers from *ca.* 0.2 to 0.06 with decreasing concentrations of [Glu(OBzl)]$_n$; the permanent dipole moment of the helix contributes more dominantly than the polarizability anisotropy to the field orientation in dilute solutions.

Since the viscosity of solvent η affects t_m, a correction factor (T/η) must be multiplied to compare values of $(t_m)_{E\to 0}$ in different solvents. By use of the limiting-low-field values of Δ_m and $(T/\eta)t_m$, together with the whole signal pattern in the reverse process, the most appropriate set of three important hydrodynamic and electric parameters [l_w, l_w/l_n, $(\beta_w)^2/2\gamma_w$] may be evaluated for each [Glu(OBzl)]$_n$ solution. The procedure for this computer-aided operation is straightforward but time-consuming. It has been described in detail in previous reports from this laboratory.[23,24] Therefore, the final result for the best three-parameter sets is given in Table I, without

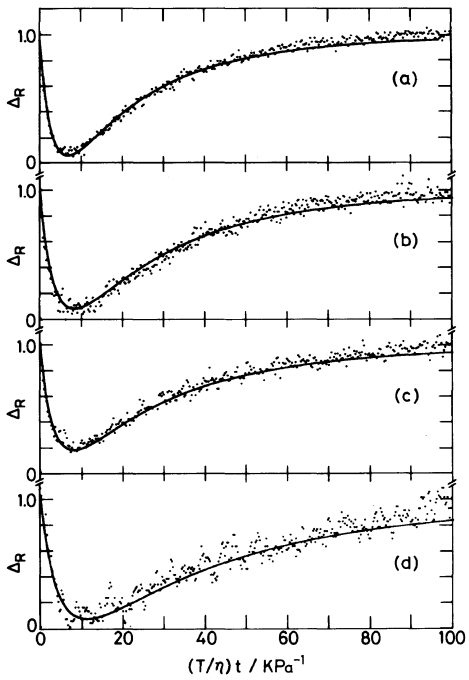

Figure 7. Observed (dots) and calculated (solid lines) reverse-transient signals of $[Glu(OBzl)]_n$ in the Kerr-law region. (a) 2-chloroethanol ($E=3.63\,kV\,cm^{-1}$, $C_p=1.12\,mM$), (b) cyclohexanone ($4.71\,kV\,cm^{-1}$, 1.54 mM), (c) pyridine ($4.84\,kV\,cm^{-1}$, 2.08 mM), and (d) chloroform ($4.00\,kV\,cm^{-1}$, 0.97 mM). Five to twenty-five signals were averaged. Ordinate: normalized birefringence signal Δ_R. Abscissa: corrected time $(T/\eta)t$.

citing the lengthy procedure here. The significance of these parameters will be discussed in the later sections.

Figure 7 shows some reverse-transient signals of $[Glu(OBzl)]_n$ in each solvent, both experimental (dots) and calculated (solid lines) with the three-parameter set in Table I. The agreement is excellent even for the chloroform solution at a dilute concentration. In this calculation, the original Broersma equation,[36]

$$\Theta_{11}(l)=\frac{1}{6\tau(l)}=\frac{3kT}{\pi\eta l^3}\left[\ln 2p-1.57+7\left(\frac{1}{\ln 2p}-0.28\right)^2\right] \quad (7)$$

was used for the rotary diffusion coefficient, where $\tau(l)$ is the relaxation time for the rotation of the whole helix molecule around the transverse axis, p is the axial ratio ($=l/2b$) with the diameter $2b$ of 17 Å for $[Glu(OBzl)]_n$.[24]

Separation of Optical and Electric Terms. Once the three-parameter set $[l_w,\ l_w/l_n,\ (\beta_w)^2/2\gamma_w]$ is evaluated, the weight-average orientation function $\langle\Phi(\beta(l),\ \gamma(l))\rangle_w$ can be calculated.[23] By fitting an experimental δ/c *vs.* E^2 curve to the theoretical curve Φ_w, plotted on a double logarithmic scale against $[(\beta_w)^2+2\gamma_w]$ or $[(\mu_w)^2+(\Delta\alpha_w/kT)]\times E^2$, three electric and optical quantities, *i.e.*, μ_w, $\Delta\alpha_w$, and $\Delta g/n$, could finally be evaluated (the curve-fitting method).[14,23] These values are also given in Table I. The results in this Table represent the electric, optical, and hydrodynamic properties of the $[Glu(OBzl)]_n$ helix in each solvent in the presence of external electric fields. The permanent dipole moment μ_w and the specific optical anisotropy factor $\Delta g/n$ are largest in cyclohexanone and smallest in pyridine. Thus, the overall helical conformation of $[Glu(OBzl)]_n$ remains almost the same in three helix-forming solvents, but the electric and optical properties are quite characteristic of individual solvents. The solvation around the periphery of helix and the specific interaction of the main-chain peptide bond and side-chain benzyl group with individual solvent molecules may all contribute to the observed difference in μ_w, $\Delta\alpha_w$, and $\Delta g/n$. Solid lines in Figure 4 are theoretical curves calculated with the values of μ_w, $\Delta\alpha_w$, and $\Delta g/n$ given in Table I. In 2-chloroethanol, cyclohexanone, and pyridine, both experimental points and theoretical curves agree quite well, indicating that the field strength dependence of steady-state birefringence can be reproduced with the parameters evaluated from the reverse-transient process. In the presence of applied electric fields, the average length of $[Glu(OBzl)]_n$ helix converges to a constant value of 1020 ± 40 Å or 1.31 ± 0.05 Å/res at dilute concentrations (*cf.* Table I).

This indicates strongly that the [Glu(OBzl)]$_n$ helix is unaggregated in the three solvents, being free from any direct effects of applied pulse fields on the conformation. The value of l_w/l_n (1.07—1.06) indicates that the distribution of chain length must be narrow in these solvents.

In chloroform, however, the agreement between experimental and calculated curves in Figure 4 is less satisfactory, probably because the structural deformation of the aggregated [Glu(OBzl)]$_n$ helix or the deaggregation of helices is induced irreversibly by applied high electric fields. The length is *ca.* 1300 Å at 3.19 mM but reduces to about 1100 Å at 0.96 mM. The notion that helices are aggregated is also supported by a large l_w/l_n value of 1.14; however, the mode of aggregation is neither simple head-to-head nor head-to-tail type.[11,21] In the former, the μ_w value would be zero for the even-numbered aggregates, while in the latter, twice as large as the μ_w value of an unaggregated helix.

It should be noted that the *field-on* build-up (or rise) process in the RPEB signal also contains valuable physical quantities,[16,20,24,27,28] and, hence, a subsequent report will show the detailed analytical procedure and comparison with results of the reverse process. Finally, it is worth pointing out that the Poisson distribution function yields nearly identical results on the molecular parameters (not shown), mostly because a fractionated [Glu(OBzl)]$_n$ sample was used in this work.[24] A more detailed study will be reported in due course on a critical comparison for the most appropriate type of distribution.

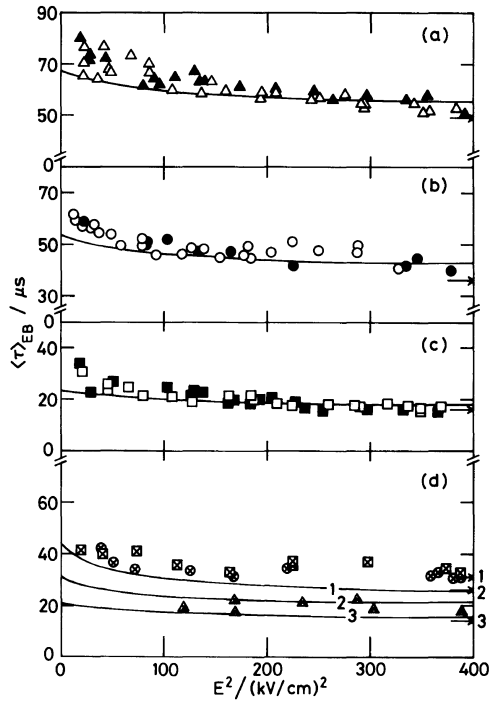

Figure 8. Electric birefringence-average relaxation time $\langle\tau\rangle_{EB}$ of [Glu(OBzl)]$_n$ *versus* the square of steady-state field strength applied to the solution before the start of the decay process. (a) 2-chloroethanol, (b) cyclohexanone, (c) pyridine, and (d) chloroform. Experimental points are represented by the same symbols as those in Figure 4. Solid lines are theoretically calculated with the field-on parameters in Table I. Horizontal arrows indicate value of τ_w at infinitely high fields. Numerals in (d) denote concentrations as 1 for 3.19 mM, 2 for 1.91 mM, and 3 for 0.96 mM.

Field-Off Process

Relaxation Time of [Glu(OBzl)]$_n$ in Decay Process. Quite independent of the field-on reverse-transient and steady-state processes, the molecular length and polydispersity, l_w and l_w/l_n, can be estimated from the field-off decay process by the mesh method.[37] This method utilizes two experimental quantities, the weight-average relaxation time τ_w and initial slope S_w. The decay process commences upon removal of an applied pulse field of arbitrary strength. The area surrounded by the normalized decay curve and baseline yields the electric birefringence-average relaxation time $\langle\tau\rangle_{EB}$ (the area method):[38,39]

$$\langle\tau\rangle_{EB}=\frac{\int_0^\infty \frac{\Phi(\beta(l),\gamma(l))lf_n(l)\mathrm{d}l}{6\Theta_{11}(l)}}{\int_0^\infty \Phi(\beta(l),\gamma(l))lf_n(l)\mathrm{d}l} \tag{8}$$

Similarly, the initial slope of the decay curve yields the electric birefringence-average initial slope $\langle S\rangle_{EB}$:[37,40]

$$\langle S\rangle_{EB}=-\frac{\int_0^\infty 6\Theta_{11}(l)\Phi(\beta(l),\gamma(l))lf_n(l)\,dl}{\int_0^\infty \Phi(\beta(l),\gamma(l))lf_n(l)\,dl} \quad (9)$$

Since $\Phi(\beta(l),\gamma(l))$ approaches unity at an infinitely high field, both $\langle\tau\rangle_{EB}$ and $\langle S\rangle_{EB}$ reduce to the weight-average relaxation time τ_w and initial slope S_w.

Figure 8 shows values of $\langle\tau\rangle_{EB}$ of $[Glu(OBzl)]_n$ in four solvents. These values are plotted against the second power of the field strength at which the electric pulse is maintained prior to the start of the decay process. In 2-chloroethanol, cyclohexanone, and pyridine, the $\langle\tau\rangle_{EB}$ *vs.* E^2 plots exhibit no marked concentration dependence. In chloroform, however, $\langle\tau\rangle_{EB}$ values show a considerable concentration dependence. By extrapolation of these $\langle\tau\rangle_{EB}$ values to infinitely high field strength, τ_w values were evaluated and are given in Table II, together with S_w values.

Both τ_w and S_w can be expressed as follows:[37]

$$\tau_w=\frac{\int_0^\infty \frac{lf_n(l)\,dl}{6\Theta_{11}(l)}}{\int_0^\infty lf_n(l)\,dl}$$
$$S_w=-\frac{\int_0^\infty 6\Theta_{11}(l)lf_n(l)\,dl}{\int_0^\infty lf_n(l)\,dl} \quad (10)$$

Hence, a theoretical mesh of the τ_w *vs.* S_w plots may be computed by use of l_w and l_w/l_n as the parameters, if both $\Theta_{11}(l)$ and $f_n(l)$ are assumed.[37] Figure 9 shows the mesh calculated on the basis of the Broersma equation for $\Theta_{11}(l)$ (*cf.* eq 7) and the Lansing-Kraemer distribution function for $f_n(l)$ (*cf.* eq 4). When paired values of τ_w and S_w, obtained experimentally for each $[Glu(OBzl)]_n$ solution, are plotted inside the mesh, the coordinates immediately give the corresponding values of l_w and l_w/l_n, which are also summarized in Table II. It should be noted that these hydrodynamic parameters were evaluated in the field-off process after removal of applied electric field.

Table II. Hydrodynamic properties of $[Glu(OBzl)]_n$ in four helix-forming solvents as evaluated from the field-off process at 20°C

Solvents[a]	τ_w / μs	$-S_w$ / μs^{-1}	l_w / Å	l_w/l_n	l_w/DP_w / Å/res
CEL	48.5	0.035	970	1.08	1.24
CHN	36.0	0.054	1000	1.10	1.28
PYN	15.3	0.130	990	1.10	1.27
CFM	31.2 (3.19)[b]	—	1500	1.14[c]	1.92
	26.2 (1.91)[b]	0.116	1390	1.16	1.78
	14.1 (0.97)[b]	0.141	1160	1.10	1.49
	11.6 (0.57)[b]	0.154	1090	1.08	1.40

[a] CEL, 2-chloroethanol; CHN, cyclohexanone; PYN, pyridine; CMF, chloroform.
[b] The value in the parentheses is the molar concentration C_p in mM.
[c] This value was obtained from the reverse signal.

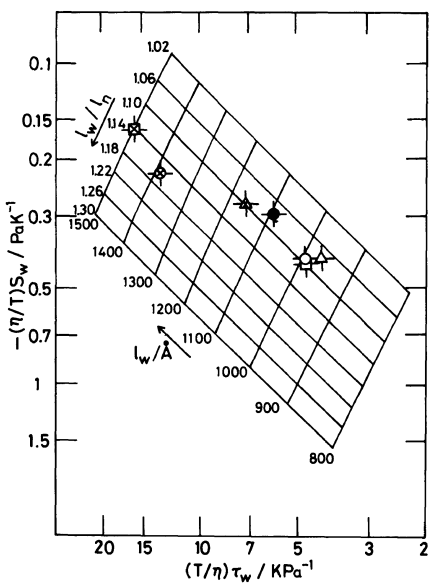

Figure 9. Theoretical meshes of $(T/\eta)\tau_w$ and $(\eta/T)S_w$ with the field-off parameters of l_w and l_w/l_n. Experimental points of $[Glu(OBzl)]_n$are (△) in 2-chloroethanol, (○) in cyclohexanone, (□) in pyridine, and (⊠, 3.19 mM; ⊗, 1.91 mM; ⧋, 0.97 mM; ●, 0.57 mM) in chloroform.

A comparison of values of l_w and l_w/l_n, obtained from the field-off decay process, with those evaluated from the field-on reverse process (Table I) makes it clear that both the axial translation of the [Glu(OBzl)]$_n$ helix and the degree of polydispersity are not affected appreciably by applied external electric fields, except for the case in chloroform.

The *field-off* $\langle\tau\rangle_{EB}$ *vs.* E^2 plots shown in Figure 8 can be calculated theoretically with the sets of the *field-on* parameters [l_w, l_w/l_n, $(\beta_w)^2/2\gamma_w$, μ_w] given in Table I. The theoretical curves are plotted with solid lines in Figure 8. Experimental points in 2-chloroethanol, cyclohexanone, and pyridine, are all in good agreement with the simulated curves within experimental error over a wide range of field strengths, especially over medium-to-high fields. Thus, it can be concluded that the hydrodynamic and electric properties, hence, the solution conformation, of molecularly dissolved [Glu(OBzl)]$_n$ helices remain almost the same in the presence and absence of an external field. This conclusion, however, cannot be applied to [Glu(OBzl)]$_n$ in chloroform at higher concentrations. The disagreement between experimental and theoretical $\langle\tau\rangle_{EB}$ *vs.* E^2 plots is obviously beyond error (3.19—0.96 mM). Hence, the external field affects not only l_w and l_w/l_n but also $(\beta_w)^2/2\gamma_w$. This result can best be interpreted as follows: in chloroform, aggregated helices are partially dissociated in the buildup process of field orientation, and thus remain in the field-on steady-state and reverse processes, but the helices tend to re-form aggregates, while being rotationally diffused in the field-off decay process.

Concentration Dependence of Relaxation Time. The apparent length of [Glu(OBzl)]$_n$ helix is longer in chloroform than in the other three solvents (*cf.* Tables I and II) at higher concentrations. Figure 10 shows the corrected relaxation time $(T/\eta)\tau_w$ and translation per residue l_w/DP_w plotted against residue concentration. In 2-chloroethanol, cyclohexanone, and pyridine, the values of $(T/\eta)\tau_w$ are

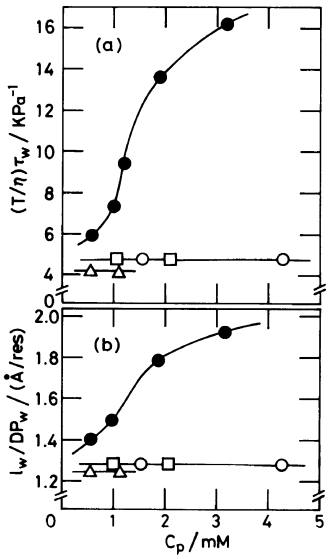

Figure 10. Concentration dependence of (a) the weight-average relaxation time corrected for the viscosity and temperature, $(T/\eta)\tau_w$, and (b) the weight-average length per residue, l_w/DP_w, of [Glu(OBzl)]$_n$. The DP_w value is taken to be 780. Solvents are (△) 2-chloroethanol, (○) cyclohexanone, (□) pyridine, and (●) chloroform.

nearly constant at about 5 kPa^{-1}, yielding values of 970—1000 Å for the length of [Glu(OBzl)]$_n$ helix in the field-off process. $(T/\eta)\tau_w$ values in chloroform vary largely in a narrow concentration range (1—3 mM), indicating that the helix transforms either from the aggregated to the molecularly dissolved species or from an elongated helical form to another compressed one below 1 mM. Both values of $(T/\eta)\tau_w$ and l_w/DP_w extrapolated to zero concentration appear to coincide with those in the other three solvents. At higher concentrations, however, the chain length is about 1500 Å. If the [Glu(OBzl)]$_n$ helix dissolved in chloroform is unaggregated at 5 mM, though unlikely,[11] the axial translation per residue, expressed by l_w/DP_w (DP_w, the weight-average degree of polymerization, is 780), would be about 1.9 Å/res, as previously observed;[14] this value is very close to that of the 3_{10}-helix.[41]

The possibility that the conformation of

$[Glu(OBzl)]_n$ in chloroform transforms from the 3_{10}-helix to the α- or ω-helix may be ruled out readily with due consideration of the electric properties given in Table I. The molecularly dissolved 3_{10}-helix should give rise to a smaller value for the permanent dipole moment μ_w than the α- or ω-helix.[42] Apparently, this is not the case, as can be seen in Table I, *i.e.*, the values of μ_w decrease with the dilution of $[Glu(OBzl)]_n$ solutions. These solutions are highly polydisperse at higher concentrations, as indicated by l_w/l_n values in Table II; hence, molecular aggregation is probably responsible for the apparently longer helix length in chloroform. In dilute solutions, l_w/DP_w values are in the range between 1.27 and 1.24 Å/res regardless of solvents for the fractionated sample used in this work. These values are also in good accord with a previous RPEB result of $[Glu(OBzl)]_n$ in *N*,*N*-dimethylformamide, in which the l_w/DP_w value was found to be 1.35 Å/res.[24] It may be concluded that the conformation of molecularly dissolved $[Glu(OBzl)]_n$ helices is nearly identical in all typical helix-forming solvents, though the electrooptical properties are solvent-specific (*cf.* Table I).

CONCLUDING REMARKS

The present RPEB study clearly shows that the overall conformation of molecularly dissolved $[Glu(OBzl)]_n$ helices in 2-chloroethanol, cyclohexanone, and pyridine is almost unaltered in the field-on ($l_w/DP_w = 1.31 \pm 0.05$ Å/res) and field-off ($l_w/DP_w = 1.25 \pm 0.02$ Å/res) processes. Thus, the applied electric pulse field orients the helices but induces no conformational transition. However, the direct field effect was evidently associated with the field orientation of aggregated helices in chloroform. This field effect is different from the one previously reported for the $[Glu(OBzl)]_n$ helix in hexafluoro-2-propanol.[26,27] In the present work, we could demonstrate that a conformational study of ordered polymers in solution by the transient electric birefringence method must be carried out with due caution. We must confirm, first of all, that a pulsed field acts on solute molecules to orient but not deform them.

The discrepancy between the l_w/DP_w value of 1.50 Å for the α-helix and that of *ca.* 1.3 Å for $[Glu(OBzl)]_n$ has already been discussed in previous papers.[24,25] At present, this finding should not be construed as an indication that the $[Glu(OBzl)]_n$ helix is in a conformation other than the α-helix (*e.g.*, the π-helix). Needless to say, l_w/DP_w values depend on the accuracy of DP_w or $\bar{M}_w$. The molecular weight *vs.* viscosity relationships so far reported were critically compared in a previous paper.[24] The disagreement between light scattering data by different investigators seems to prevent a precise determination of $\bar{M}_w$ values from the intrinsic viscosity. Thus, a new, definitive $\bar{M}_w$ *vs.* $[\eta]$ relationship must be available, before a clear-cut conclusion is reached on the conformation of $[Glu(OBzl)]_n$.

Re-investigation of the absolute molecular weight by light scattering is desirable. At the same time, the adequacy of the original Broersma equation for the rotary diffusion coefficient Θ_{11} should be critically reviewed with a monodispersed rodlike sample of known molecular weight. The molecular weight distribution pattern may be determined by an independent method, *e.g.*, gel permeation chromatography; then, the most appropriate form of distribution function can be selected for $f_n(l)$. Still more important, the polymer samples should be fractionated, for example, by the successive precipitation method which is relatively simple but quite effective to narrow the molecular weight distribution. Together with these "pretreatments" of polymer samples of known absolute molecular weights (preferably the weight-averaged one by light scattering), the square-wave and reversing-pulse electric birefringence techniques can be utilized with confidence to resolve the conformation of various polymers in solution. The present

work has fully detailed the merits of these transient RPEB techniques.

Acknowledgements. We thank Prof. R. Sakamoto of Gifu University for his suggestions regarding solvent choice and his allowing us use of his manuscript for reference.

REFERENCES

1. S. Yamamoto and K. Yamaoka, *Polym. Prepr. Jpn.*, **32**, 2385 (1983).
2. P. Doty, J. H. Bradbury, and A. M. Holtzer, *J. Am. Chem. Soc.*, **78**, 947 (1956).
3. V. Luzzati, M. Cesari, G. Spach, F. Masson, and J. M. Vincent, "Polyamino Acids, Polypeptides, and Proteins," M. A. Stahmann, Ed., Univ. Wisconsin Press, Wisconsin, OH, 1962, pp 121—130.
4. G. Spach, L. Freund, M. Daune, and H. Benoit, *J. Mol. Biol.*, **7**, 468 (1963).
5. H. Fujita, A. Teramoto, K. Okita, T. Yamashita, and S. Ikeda, *Biopolymers*, **4**, 769 (1966).
6. H. Fujita, A. Teramoto, T. Yamashita, K. Okita, and S. Ikeda, *Biopolymers*, **4**, 781 (1966).
7. V. N. Tsvetkov, I. N. Shtennikova, V. S. Skazka, and E. I. Rjumtsev, *J. Polym. Sci., C*, **16**, 3205 (1968).
8. J. Lilie, J. Springer, and K. Ueberreiter, *Kolloid Z.-Z. Polym.*, **226**, 138 (1968).
9. J. P. Kratohvil, *Kolloid Z. Z. Polym.*, **238**, 455 (1970).
10. K. Kubota and B. Chu, *Biopolymers*, **22**, 1461 (1983).
11. R. Sakamoto and M. Watanabe, "Contemporary Topics in Polymer Science," Vol. 4, W. J. Bailey and T. Tsuruta, Ed., Plenum Press, New York, N.Y., 1984, pp 259—268.
12. C. Tanford, "Physical Chemistry of Macromolecules," Wiley, New York, N.Y., 1961, pp 333—343 and 390—412, Chapter 6.
13. C. T. O'Konski, K. Yoshioka, and W. H. Orttung, *J. Phys. Chem.*, **63**, 1558 (1959).
14. K. Yamaoka, Ph. D. Dissertation, University of California, Berkeley, CA, 1964.
15. K. Yoshioka, "Molecular Electro-Optics," Part 2, C. T. O'Konski, Ed., Marcel Dekker, New York, N.Y., 1978, pp 601—643, Chapter 17. Numerous references are cited therein prior to 1974.
16. E. Fredericq and C. Houssier, "Electric Dichroism and Electric Birefringence," Clarendon Press, Oxford, 1973.
17. K. Yamaoka, "Kobunshidenkaishitsu (Polyelectrolytes), Kobunshi Jikkengaku," Vol. 13, ed., Kyoritsu Publishing Co., Tokyo, 1978, pp 239—255.
18. H. Watanabe, "Seitaikobunshi (Biopolymers), Kobunshi Jikkengaku," Vol. 14, ed., Kyoritsu Publishing Co., Tokyo, 1984, pp 54—74.
19. H. Watanabe, K. Yoshioka, and A. Wada, *Biopolymers*, **2**, 91 (1964).
20. K. Nishinari and K. Yoshioka, *Kolloid Z. Z. Polym.*, **240**, 831 (1970).
21. W. Pyżuk and T. Krupkowski, *Makromol. Chem.*, **178**, 817 (1977).
22. I. Tinoco, Jr. and K. Yamaoka, *J. Phys. Chem.*, **65**, 423 (1959).
23. K. Yamaoka and K. Ueda, *J. Phys. Chem.*, **86**, 406 (1982).
24. K. Ueda, M. Nomura, and K. Yamaoka, *Biopolymers*, **22**, 2077 (1983).
25. K. Ueda, M. Mimura, and K. Yamaoka, *Biopolymers*, **23**, 1667 (1984).
26. K. Ueda and K. Yamaoka, *Polym. Prepr. Jpn.*, **33**, 2911 (1984). Part of work was presented at the 34th meeting of the Society of Polymer Science, Japan, held at Sendai, Sept., 1984.
27. K. Ueda, *Bull. Chem. Soc. Jpn.*, **57**, 2703 (1984).
28. K. Yamaoka, S. Yamamoto, and K. Ueda, *J. Phys. Chem.*, **89**, 5192 (1985).
29. K. Yamaoka, T. Ichibakase, K. Ueda, and K. Matsuda, *J. Am. Chem. Soc.*, **102**. 5109 (1980).
30. E. Scoffone, E. Peggion, A. Cosani, and M. Terbojevich, *Biopolymers*, **3**, 535 (1965).
31. K. Yamaoka and K. Matsuda, *J. Sci. Hiroshima Univ. Ser. A*, **43**, 185 (1980).
32. K. Yamaoka and K. Ueda, *Bull. Chem. Soc. Jpn.*, **56**, 2390 (1983).
33. A. Peterlin and H. A. Stuart, "Hand- und Jahrbuch der Chemischen Physik," Bd. 8, von A. Eucken and K. L. Wolf, Ed., Abt. IB, Akad. Verlagsges., Leipzig, 1943, pp 1—115.
34. W. D. Lansing and E. O. Kraemer, *J. Am. Chem. Soc.*, **57**, 1369 (1935).
35. P. J. Flory, *J. Am. Chem. Soc.*, **62**, 1561 (1940).
36. S. Broersma, *J. Chem. Phys.*, **32**, 1626 (1960).
37. K. Yamaoka and K. Fukudome, *Bull. Chem. Soc. Jpn.*, **56**, 60 (1983).
38. K. Yoshioka and H. Watanabe, *Nippon Kagaku Zasshi*, **84**, 626 (1963).
39. K. Yoshioka and H. Watanabe, "Physical Principles and Techniques of Protein Chemistry," Part A, S. J. Leach, Ed., Academic Press, New York, N.Y., 1969, pp 335—367, Chapter 7.
40. M. Matsumoto, H. Watanabe, and K. Yoshioka, *Biopolymers*, **11**, 1711 (1972).
41. R. E. Dickerson and I. Geis, "The Structure and Action of Proteins," Harper & Row, New York, N.Y., 1969, pp 24—43, Chapter 2.
42. A. Wada, "Advances in Biophysics," Vol. 9, M. Kotani, Ed., Japan Scientific Societies Press, Tokyo, 1976, pp 1—63.